Doxorubicin Liposome-Loaded Microbubbles for Contrast Imaging and Ultrasound-Triggered Drug Delivery

Jean-Michel Escoffre,* *Member, IEEE*, Christophoros Mannaris,* Bart Geers, Anthony Novell, *Member, IEEE*, Ine Lentacker, Michalakis Averkiou, *Senior Member, IEEE*, and Ayache Bouakaz, *Senior Member, IEEE*

***Abstract*—Targeted drug delivery under image guidance is gaining more interest in the drug-delivery field. The use of microbubbles as contrast agents in diagnostic ultrasound provides new opportunities in noninvasive image-guided drug delivery. In the present study, the imaging and therapeutic properties of novel doxorubicin liposome-loaded microbubbles are evaluated. The results showed that at scanning settings (1.7 MHz and mechanical index 0.2), these microbubbles scatter sufficient signal for nonlinear ultrasound imaging and can thus be imaged in real time and be tracked *in vivo*. *In vitro* therapeutic evaluation showed that ultrasound at 1 MHz and pressures up to 600 kPa in combination with the doxorubicin liposome-loaded microbubbles induced 4-fold decrease of cell viability compared with treatment with free doxorubicin or doxorubicin liposome-loaded microbubbles alone. The therapeutic effectiveness is correlated to an ultrasound-triggered release of doxorubicin from the liposomes and an enhanced uptake of the free doxorubicin by glioblastoma cells. The results obtained demonstrate that the combination of ultrasound and the doxorubicin liposome-loaded microbubbles can provide a new method of noninvasive image-guided drug delivery.**

I. Introduction

Doxorubicin (DOX) is one of the most powerful anticancer drugs prescribed on its own or in combination with other agents. Because of its broad spectrum of activity, it is widely used for the treatment of solid tumors and hematological malignancies [1]. However, the use of free DOX in clinical application is still rather limited because of the severe systemic side effects associated with its use. To overcome these major problems, DOX has been encapsulated inside pegylated liposomes, preventing their recognition by the reticuloendothelial system [2]. This formulation results in the passive accumulation of liposomes in the leaky tumor vasculature because of the enhanced permeability and retention effect [3]. Doxil, a clinically approved liposomal DOX formulation, is currently indicated for the treatment of cancers such as Kaposi's sarcoma and ovarian cancer [2], [4]. Although Doxil strongly reduced the cardiotoxicity of DOX in clinical trials [5], other adverse effects have been reported, such as patients suffering from mucositis and hand and foot syndrome resulting from the localization of liposomes in skin capillaries [6]. Both the pharmacological actions of DOX and its toxicological effects are related to tissue concentration of DOX [1]. For that reason, the development of a more efficient and targeted delivery method is required to increase the local concentration of DOX at the desired site while minimizing side effects to healthy tissues.

Image-guided ultrasound-mediated drug delivery shows great promise in improving the therapeutic ratio of a chemotherapeutic agent by increasing the local deposition and reducing the systemic side effects [7]–[9]. The combination of ultrasound waves and ultrasound contrast agents (microbubbles) is known to enhance the vascular extravasation and the intracellular delivery of drugs [10]–[14]. The exposure of microbubbles to ultrasound causes the expansion and the contraction of microbubbles during the respective rarefaction and compression phases of the ultrasound wave. These oscillations may cause liquid flow around the microbubbles, known as microstreaming [15], [16]. At even higher acoustic pressures, the microbubbles undergo large oscillations, which lead to violent collapse and destruction of the microbubbles and in some cases inertial cavitation, wherein the microbubble disruption might be accompanied by the generation of shock waves in the medium close to the microbubbles [17]. In the case of an asymmetrical collapse, jet formation may also occur when a collapsing microbubble is located near the cell membrane [18]. These different physical phenomena can transiently enhance the permeability of tumor vasculature and cells and, therefore, the extravasation and the intracellular uptake of the drugs [19], [20].

A key component of ultrasound-triggered local drug delivery is the ability to image the drug delivery vehicle in real time. Ideally, the drug carrier should be able to be tracked *in vivo* using low-mechanical-index (MI) imaging and once at the desired location, high-MI ultrasound may be used to trigger the drug release on site. Another approach is to image the microbubble destruction process with Doppler-based methods [21].

Manuscript received February 24, 2012; accepted June 7, 2012. This project was funded by the EU/FP7 Project Sonodrugs (NMP4-LA-2008-213706).

*J-M. Escoffre and C. Mannaris have contributed equally to this work.

J.-M. Escoffre, A. Novell, and A. Bouakaz are with the UMR Imagerie et Cerveau, INSERM U930, and Université François Rabelais, Tours, France (e-mail: ayache.bouakaz@univ-tours.fr).

C. Mannaris and M. Averkiou are with the Department of Mechanical and Manufacturing Engineering, University of Cyprus, Nicosia, Cyprus.

B. Geers and I. Lentacker are with the Laboratory of General Biochemistry and Physical Pharmacy, Department of Pharmaceutics, Ghent University, Ghent, Belgium.

DOI http://dx.doi.org/10.1109/TUFFC.2013.2539

Several studies reported on the synergistic effect of DOX and ultrasound. These studies focused mainly on the intracellular delivery of free or encapsulated DOX by ultrasound alone [22]–[25] or co-injected with contrast agent [26]–[29]. However, a major limitation of the co-administration approach is that liposomes can still extravasate and accumulate in untargeted tissues, such as the skin capillaries, resulting in undesired side effects [6]. To minimize this side effect, one strategy is to develop a drug-loaded microbubbles [26], [30], [31]. Geers *et al.,* designed doxorubicin liposomes-loaded microbubbles. Hence, the DOX is encapsulated in liposome particles that bind to the lipid shell of the microbubbles through a covalent link [26]. The clinical potential of the DOX liposome-loaded microbubbles rests on ultrasound-triggered DOX delivery monitored by ultrasound contrast imaging.

The goal of this study was first to investigate the imaging characteristics of the liposome-loaded microbubbles and to compare their performance to those of a commercially available contrast agent (SonoVue, Bracco Research, Geneva, Switzerland). Then, the therapeutic effectiveness of the DOX liposome-loaded microbubbles in human glioblastoma cells was evaluated and the mechanism of DOX delivery was investigated.

II. Material and Methods

A. Preparation of Microbubbles

1) Unloaded Microbubbles: Unloaded microbubbles were prepared via the method described by Geers *et al.* [26]. Briefly, microbubbles were prepared from a lipid solution of 1,2-dipalmitoyl-sn-glycero-3-phosphocholine (DPPC) and 1,2-distearoyl-sn-glycero-3-phosphoethanolamine-N-[PDP(polyethylene glycol)-2000] (DSPE-PEG-PDP) (Avanti Polar Lipids, Albaster, AL) in a 1:2:7 glycerine-propyleneglycol-H_2O solvent (Sigma-Aldrich, Bornem, Belgium). The molar ratio of the lipids in the lipid solutions was, respectively, 65:35. This lipid solution was prepared as follows: the different lipids dissolved in $CHCl_3$ were mixed and the solvent was evaporated. Afterward, the remaining lipid-film was dissolved in glycerine-propyleneglycol-H_2O. One milliliter of the mixture was transferred to a glass vial and its headspace was filled with C_4F_{10} gas (F2 Chemicals, Preston, UK) before mechanical agitation. Finally, unloaded microbubbles were obtained by high-speed shaking of the lipid solution in a Capmix device (3M-ESPE, Diegem, Belgium) for 15 s. The size and the concentration of the microbubbles in the dispersion (i.e., number of microbubbles/microliter) were determined with a Beckman-Coulter Multisizer 4 (Beckman-Coulter, Brea, CA). The unloaded microbubbles showed an average volume diameter of 3.6 μm. The microbubble dispersions contained 1.23×10^9 microbubbles/mL.

2) DOX Liposome-Loaded Microbubbles: DOX liposome-loaded microbubbles were prepared by adding adequate amounts of DOX liposomes functionalized with DSPE-PEG-MALEIMIDE (Avanti Polar Lipids) to the lipid-solution before mechanical activation (Fig. 1). The DOX-liposomes were prepared via the method described by Lentacker *et al.* [32]. Briefly, adequate amounts of DPPC, DSPE-PEG-MALEIMIDE and cholesterol (dissolved in $CHCl_3$) were transferred to a round-bottom flask and the solvent was evaporated using a rotary evaporator. The remaining lipid-film was then hydrated with ammonium sulfate buffer (250 mM) and the liposomal solution was extruded through a 200-nm filter. To remove the excess of ammonium sulfate, the liposome dispersion was pelletized in a Beckman L8-M ultracentrifuge at 10 000 g. Finally, DOX liposomes were obtained by incubating the obtained liposomal dispersion with a sufficient amount of DOX in HCl (10 mg/mL in H_2O) at 50°C for 2 h. Afterward, the nonencapsulated DOX was removed by ultracentrifugation at 10 000 g (Beckman L8-M ultracentrifuge). Finally, adequate amounts of DOX-liposomes were mixed with the (DPCC, DSPE-PEG-SPDP) lipid solution as described in the previous section and were transferred into glass vials and its headspace was filled with C_4F_{10}. After 15 s of mechanical agitation, the loaded microbubbles showed an average volume diameter of 4 μm. The microbubble dispersions contained approximately 1.04×10^9 microbubbles/mL.

B. Acoustic Characterization

1) Microbubble Imaging: In this section, the imaging characteristics of the unloaded microbubbles and DOX liposome-loaded microbubbles were investigated and compared with SonoVue using the setup shown in Fig. 2. The microbubbles were diluted to a concentration of 0.2‰ (0.2 mL of contrast agent in 1 L of deionized water), which lies in the low end of the linear range of the

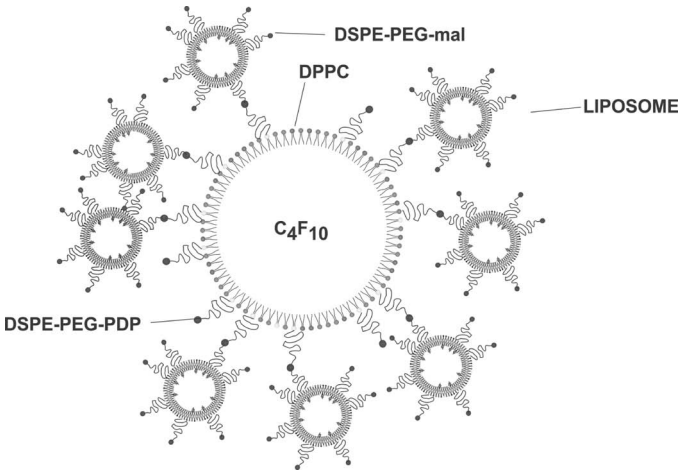

Fig. 1. Schematic presentation of doxorubicin (DOX) liposome-loaded microbubbles. The microbubbles are filled with the hydrophobic C_4F_{10} gas. DOX-containing liposomes are coupled to the microbubble's surface through covalent thiol-maleimide linkages. The DOX liposome-loaded microbubbles showed an average volume diameter of 4 μm, whereas the DOX-loading liposomes are 200 nm in diameter.

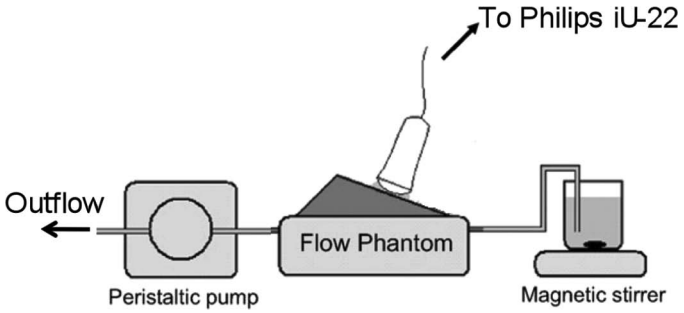

Fig. 2. Flow phantom setup. A peristaltic pump draws the samples into a tissue-mimicking flow phantom (attenuation coefficient 0.5 dB/cm per MHz). Imaging done by a C5–1 curvilinear transducer and a Philips iU-22 ultrasound scanner.

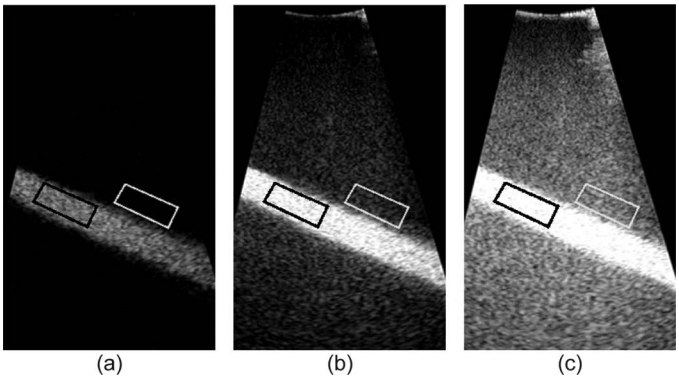

Fig. 3. Selection of regions of interest in QLAB for contrast-to-tissue ratio (CTR) calculation at mechanical indices (MIs) of (a) 0.05, (b) 0.3, and (c) 0.7. Two identical regions were selected at the same depth, one inside the tube lumen (contrast) and one outside the tube (tissue).

relation of intensity versus concentration [33], and this is similar to what is usually used clinically (normally 2.4 mL injected in 5 L of blood) [21]. The original concentration of all three types of microbubbles used in this study is 10^8 microbubbles/mL; thus, consistency was maintained. The solution was continuously mixed by a magnetic stirrer to avoid flotation and to ensure uniform distribution of the microbubbles while a peristaltic pump (Masterflex, Cole-Palmer, Vernon Hills, IL) was used to draw the solution into a rubber-based tissue mimicking cardiac Doppler-flow phantom (Model 523A, ATS Laboratories Inc., Bridgeport, CT). Contrast-enhanced ultrasound imaging of the microbubbles was performed with the C5–1 curvilinear transducer of a Philips iU-22 (Philips Medical Systems, Bothell, WA) ultrasound scanner. The transducer was placed so as to image the 8-mm-diameter flow channel of the phantom at a depth of 12 cm. A power modulation nonlinear pulsing scheme [34], [35] was used at a transmit center frequency of 1.7 MHz.

The contrast-to-tissue ratio (CTR) under different excitation pressures was measured using the setup described above. CTR is defined as the ratio of the scattered intensity from the microbubbles to the scattered intensity from tissue and it is an index of the ability to image contrast agent in the presence of tissue. Acoustic pressures ranging from 0.06 to 0.98 MPa, corresponding to mechanical indices (MI) of 0.05 to 0.75 were used. A continuous infusion of the microbubble solution was passed through the phantom and 5 frames per MI were acquired at a frame rate of 0.5 Hz. The total volume in the field of view was about 5 mL (radius = 4 mm, length = 10 cm), so a flow rate of 200 mL/min (6.7 mL in 2 s) was used to make sure the region of interest (ROI) was refreshed with new microbubbles for each frame so that microbubble destruction would not be an issue. QLAB software (Philips Healthcare, Andover, MA) was used in the analysis of the data. QLAB allows for selection of one or more ROIs and produces time–intensity curves from the image loops. The intensity is obtained from uncompressed envelope detected data squared and then averaged from all pixel values in the ROI. Two ROIs were selected, one inside the tube lumen and one outside the tube. CTR as a function of MI was obtained by dividing the backscattered intensity from the microbubbles by the backscattered intensity from tissue (in absolute scale units). In Fig. 3, examples of the ROI selection during a CTR experiment are shown for low, medium, and high MI.

2) Microbubble Destruction: The setup shown in Fig. 2 was also used to investigate the destruction of the unloaded and DOX liposome-loaded microbubbles when exposed to ultrasound at MIs of 0.05 to 0.75. The destruction threshold of the microbubbles would allow us to determine the optimal MI to image and track the microbubbles *in vivo* without causing destruction and premature release of the drug, as well as to optimize the imaging of the microbubble destruction process with a Doppler-based method. Similar to the CTR experiments, the results were compared with SonoVue.

A freshly made solution of microbubbles (C = 0.2‰) was pumped into the flow phantom and the flow was stopped. The microbubbles were then insonified for 10 s at a frame rate of 10 Hz (100-ms interval). The 10 s imaging duration was selected so that it would be long enough to determine the ultrasound effect on the microbubbles (rate of destruction) while at the same time short enough to avoid any microbubble flotation. QLAB was used to select a single ROI in the middle of the tube, and the decrease in intensity as a function of time was measured.

C. DOX Delivery by Microbubble-Assisted Ultrasound

1) Cell Culture: Human glioblastoma cells (U-87 MG) were derived from a malignant glioma [European Collection of Cell Cultures (ECACC), Salisbury, UK]. Cells were grown as a monolayer in Dulbecco's Modified Eagle's Medium (DMEM; Gibco-Invitrogen, Carlsbad, CA) supplemented with 10% heat-inactivated fetal calf serum (FCS; Gibco-Invitrogen). The cells were routinely subcultured every 4 d and incubated at 37°C in humidified atmosphere with a 5% CO_2 incubator.

2) Ultrasound Setup: Ultrasound waves were generated from a single-element transducer with a center fre-

quency of 1 MHz. The 13-mm-diameter transducer was focused at 30 mm with a wide focal spot (i.e., beamwidth at −6 dB = 5 mm). The transducer was driven with an electrical signal generated by an arbitrary waveform generator (Agilent Technologies Inc., Santa Clara, CA) and amplified with a power amplifier (ADECE, Artannes sur Indre, France). The peak negative pressure of the acoustic wave was measured in a separate setup using a calibrated PVDF needle hydrophone (0.2 mm diameter, Precision Acoustics, Dorchester, UK) at the natural focal distance of the transducer.

3) DOX Delivery: U-87 MG cells were trypsinized, washed once, and resuspended in OptiMEM (Gibco-Invitrogen) supplemented with 1% FCS. During the procedure, the cell suspension was maintained in a water bath at 37°C (Grant Instruments Ltd., Cambridge, UK). The cell suspension (3×10^5 cells in 1.5 mL) was then placed in a polystyrene cuvette (45 mm height, 10 mm inside diameter, 12 mm outside diameter; Fisher Scientific SAS, Illkirch, France) and 15 μL of unloaded microbubbles alone or DOX liposome-loaded microbubbles were added just before ultrasound application. Thus, a microbubble-cell ratio of 5 was achieved and the final concentration of DOX was of 3 μg/mL. The center of the plastic cuvette was positioned at the focal distance of the transducer in a deionized water tank at 37°C. The cell suspension was kept uniform through a gentle magnetic stirring during ultrasound application. Subsequently, the cell suspension was exposed to 1-MHz sinusoidal ultrasound waves with a pulse repetition period of 100 μs, 40 cycles per pulse and for 30 s (i.e., optimal acoustic parameters for gene and drug delivery, as determined by Escoffre *et al.* [27]). The applied acoustic pressures were 200 to 600 kPa.

After ultrasound application, 500 μL of cells were cultured in 24-well cell culture plates (Corning Life Science BV, Amsterdam, The Netherlands) and incubated at 37°C in a humidified atmosphere with a 5% CO_2 incubator. Four hours later, 1 mL of OptiMEM-10% FCS was added to each well and incubated at 37°C in humidified atmosphere with a 5% CO_2 incubator for 48 h.

4) DOX Uptake: Forty-eight hours after ultrasound-triggered DOX delivery, the cell medium was removed and the cells were washed with PBS and collected through centrifugation (i.e., 3 min, 800 *g*). The cells were resuspended in 500 μL of PBS. Fluorescence histograms were recorded with a flow cytometer (Beckman-Coulter, Fullerton, CA) and analyzed using the Kaluza software supplied by the manufacturer. A minimum of 10 000 events was analyzed to generate each histogram. The gate was arbitrarily set for the detection of red fluorescence [27].

5) DOX Release: The experimental procedure was adapted from de Smet *et al.,* 2010 [36] and performed at 37°C. The DOX release from DOX liposomes or DOX liposome-loaded microbubbles was determined by measuring the intensity of fluorescence (λ_{ex} = 485 nm and λ_{em} = 590 nm) at 37°C and 10 min after treatment. A volume of 15 μL of unloaded microbubbles alone or DOX liposome-loaded microbubbles was added to the plastic cuvette containing 1.5 mL of OptiMEM-1% FCS just before ultrasound application. Subsequently, the solution was exposed to ultrasound. Three experimental groups were selected: 1) DOX liposomes or DOX liposome-loaded microbubbles after Triton X-100 at 10% v/v, which induces DOX release by dissolving the liposomes (positive control); 2) DOX liposomes or DOX liposome-loaded microbubbles alone (negative control); and 3) Combination of DOX liposomes or DOX liposome-loaded microbubbles with ultrasound. After ultrasound application, 150 μL of the solution was introduced into a 96-well plate (Corning Life Science BV). The percentage of DOX release was calculated according to

$$\text{DOX release (\%)} = \frac{I_{\text{exp}}}{I_{100}} \times 100,$$

in which I_{100} and I_{exp} are, respectively, the fluorescence intensity of positive control and the negative control or the combination of DOX liposome-loaded microbubbles with ultrasound.

6) Cell Viability: The cell viability was evaluated using an MTT assay. Forty-eight hours after treatment, the cell medium was replaced with 0.5 mg/mL MTT solution (Molecular Probes, Invitrogen) and the cells were incubated at 37°C in humidified atmosphere with a 5% CO_2 incubator for 1.5 h. Afterwards, the MTT solution was substituted by the DMSO solution (Sigma-Aldrich, St. Louis, MO) and the cells were incubated for 10 min under gentle agitation at room temperature. The absorbance was then measured at 570 nm (OD_{570}) to determine the amount of formed formazan and at 690 nm (OD_{690}) as a reference. The cell viability (CV) was calculated as [32]

$$\text{CV} = \frac{(\text{OD}_{570}x - \text{OD}_{690}x)}{(\text{OD}_{570}\ \text{control} - \text{OD}_{690}\ \text{control})} \times 100.$$

7) Statistical Analysis: Data are presented as mean ± standard error of the mean (SEM) of five independent experiments. Statistical analysis was performed using the nonparametric Mann-Whitney test. Significance was defined as $p < 0.05$ (NS, non-significance; $^*p < 0.05$; $^{**}p < 0.01$; $^{***}p < 0.001$).

III. Results

A. Ultrasonic Characterization

In this section, the measurements of CTR and destruction properties of the microbubbles are presented.

1) Contrast-to-Tissue Ratio: The contrast-to-tissue ratio for SonoVue as a function of the MI as well as the

scattered intensity is shown in Fig. 4(a) (uncompressed data shown in decibels). The backscattered intensity from microbubbles (ROI inside the tube) is shown in black (line with solid dots) and for tissue (ROI outside the tube) in blue (line with crosses). The calculated CTR is shown in red (line with squares). SonoVue microbubbles exhibit a higher CTR at low, non-destructive MIs. At MIs of 0.05 and 0.1, the CTR reaches 22 and 27 dB respectively. The best CTR for this setting of the ultrasound scanner is found at MI = 0.2 (29 dB). At this setting however, the pressure is high enough to destroy the microbubbles and real-time imaging is not possible [real-time contrast imaging with Sonovue is carried out at non-destructive pressures (MI < 0.1)]. At higher MIs, incomplete tissue cancellation resulting from nonlinear propagation of ultrasound causes the tissue signal to increase considerably, whereas the corresponding increase in the microbubble signal is less. As a result, the overall CTR decreases. The white area indicates the non-destructive MIs, and the gray area, the destructive MIs.

The CTR for unloaded microbubbles is shown in Fig. 4(b). CTRs of 13 and 18 dB are measured for nondestructive MIs of 0.05 and 0.1, respectively. Even though these are 9 dB less than SonoVue, there is still enough microbubble signal for imaging. The best CTR for these scanning settings is 25 dB and it is reached at MI = 0.26. Similar to SonoVue, the CTR decreases at higher MIs. Bubble size, concentration, gas content, frequency, shell elasticity, and thickness are among the various parameters influencing the microbubble response (and consequently the CTR).

Loading of the microbubbles with the DOX-liposomes does not seem to have an impact on the imaging properties of the microbubble; the results for DOX liposome-loaded microbubbles [shown in Fig. 4(c)] are nearly identical to the results of the unloaded microbubbles shown in Fig. 4(b). One small difference is that loading of the microbubbles with DOX-liposomes seems to make them a slightly tougher and the destruction threshold (as described in the next section) increases. Real-time non-destructive imaging at this optimal setting (CTR = 25 dB) may be possible with the drug-loaded microbubbles.

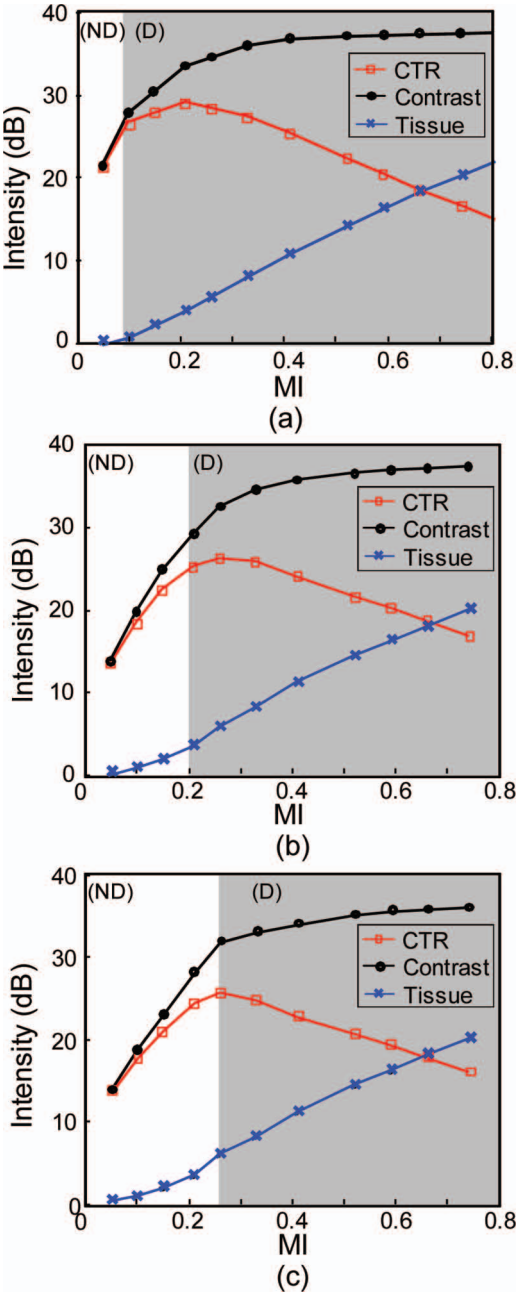

Fig. 4. Contrast-to-tissue ratio for (a) SonoVue microbubbles, (b) unloaded microbubbles, and (c) doxorubicin (DOX) liposome-loaded microbubbles. The backscattered intensity from microbubbles [region of interest (ROI) inside the tube] is shown in black (line with solid dots) and for tissue (ROI outside the tube) in blue (line with crosses). The calculated contrast-to-tissue ratio (CTR) is shown in red (line with squares). The white area indicates the non-destructive mechanical indices (MIs), and the gray area, the destructive MIs.

2) Microbubble Destruction: The microbubble destruction patterns for various MIs are shown in Fig. 5. The time axis is given in seconds and the signal intensity in arbitrary intensity units (AIU). MIs of 0.05, 0.1, 0.21, 0.33, and 0.41 were used and ultrasound was applied for 6 s (60 frames). Higher pressures and longer exposure times followed the same trends (data not shown). The destruction of SonoVue microbubbles is shown in Fig. 5(a). At MI 0.05, the intensity remains constant throughout the insonation period, indicating that there is no destruction, whereas at MI 0.1, the intensity gradually decreases, indicating that destruction is taking place. More than 6 s (60 frames) are required for the overall intensity to drop to half its initial value. Higher pressures steadily become more destructive, as expected, and at MI 0.4 the majority of the bubbles are destroyed within 2 to 3 s.

Fig. 5(b) demonstrates the destruction patterns of unloaded microbubbles. Unlike SonoVue, the scattered intensity at MI of 0.1 remains constant throughout the insonation period, indicating that there is no destruction. Destruction is first observed at MI 0.21, where in the first second, the intensity drops by a factor of 2 before reach-

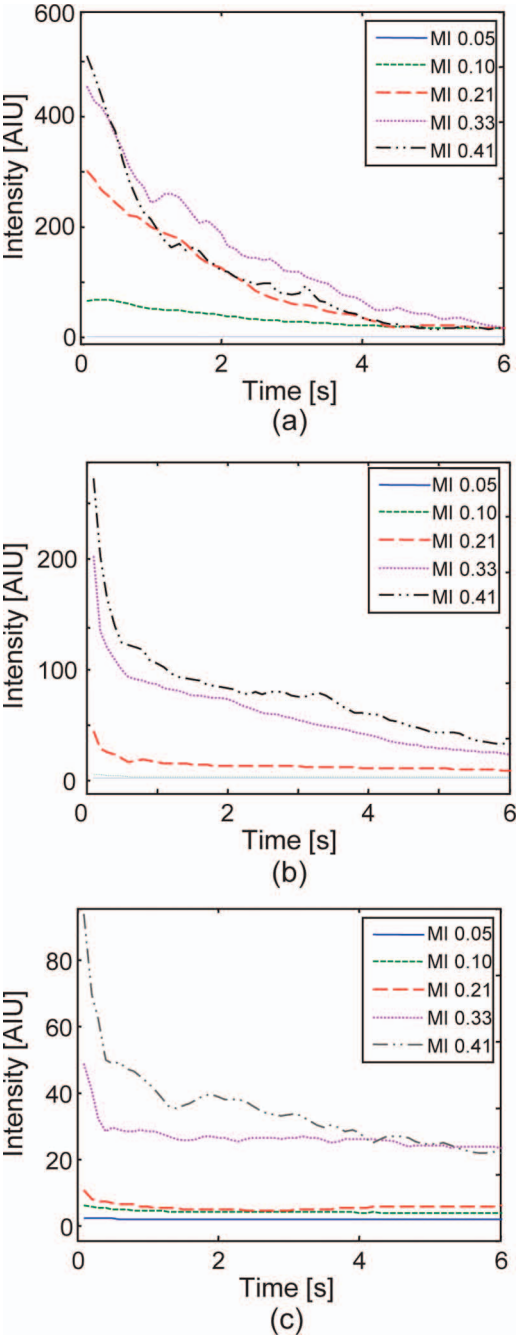

Fig. 5. Kinetics of destruction of (a) SonoVue microbubbles, (b) unloaded microbubbles, and (c) doxorubicin (DOX) liposome-loaded microbubbles. Mechanical indices (MIs) of 0.05, 0.1, 0.21, 0.33, and 0.41 are applied for 6 s (60 frames).

ing steady state. At higher MIs, a sudden drop in the scattered intensity within the first 5 to 6 frames, followed by a constant decay throughout the insonation period is observed.

The corresponding results for DOX liposome-loaded microbubbles are shown in Fig. 5(c). Similar to the unloaded microbubbles, MIs of 0.05 and 0.10 are nondestructive; the intensity remains constant throughout the insonation time. MI 0.21 is slightly destructive because a slight decrease in intensity is observed in the first 4 to 5 frames. Clear destruction can be seen at MI 0.33, for which the intensity drops to 50% of its initial value within 4 to 6 frames before reaching a plateau. Similar trends were observed at higher MIs.

B. Evaluation of Therapeutic Efficiency and Mechanism of Drug Delivery

1) Enhancement of DOX-Induced Glioblastoma Cell Death by DOX Liposome-Loaded Microbubbles and Ultrasound: Cell viability was assessed by the MTT assay 48h after treatment with DOX liposome-loaded microbubbles and ultrasound and the results are shown in Fig. 6. When the U-87 MG cells were insonated at 600 kPa (MI = 0.6) with only the presence of unloaded microbubbles, the cell viability was 87 ± 2% (Fig. 6). Similar cell viability was obtained at 200 and 400 kPa with the unloaded microbubbles. As shown in Fig. 6, the cell viability after treatments with free DOX and DOX liposomes-loaded microbubbles alone were 67 ± 1% and 71 ± 1%, respectively. The cytotoxicity induced by the treatment with DOX liposome-loaded microbubbles alone can be ascribed to the presence free DOX-liposomes in the vial after mechanical activation, which can be endocytosed by the cells causing thus cytotoxicity. The combination of DOX liposome-loaded microbubbles and ultrasound at 200 kPa induced a 2-fold decrease of cell viability compared with free DOX or DOX liposome-loaded microbubbles alone ($***p < 0.001$).

Increasing the acoustic pressure to 400 and 600 kPa caused a 3- and 4-fold decrease of cell viability respectively when compared with free DOX or DOX liposome-loaded microbubbles alone ($***p < 0.001$). These results clearly showed that the combination of DOX liposome-loaded microbubbles with ultrasound induced a synergistic effect on the U-87 MG cell death.

2) Enhancement of DOX Release From DOX Liposome-Loaded Microbubbles After Insonation: Because of the high intra-liposomal DOX amount, the native DOX fluorescence is quenched. Release of DOX from the aqueous intra-liposomal medium will result in the dilution of the free DOX in the extra-liposomal medium, leading to an increment of fluorescence intensity. The latter is proportional to the amount of DOX in the medium. The DOX release was assessed by spectrofluorometry after insonation of DOX liposome-loaded microbubbles. The insonation at 600 kPa of DOX liposome-loaded microbubbles induced a significant increase of DOX release from the liposomes loaded on the microbubbles ($***p < 0.001$ compared with the incubation of DOX-loaded microbubbles in the medium of cell culture; Fig. 7). These results reveal that the combination of DOX liposome-loaded microbubbles with ultrasound induced an active release of doxorubicin from liposomes.

3) Enhancement of DOX Uptake by DOX Liposome-Loaded Microbubbles and Ultrasound: Flow cytometry was used for quantitative determination of DOX uptake in the U-87 MG glioblastoma cells. The native fluorescence of

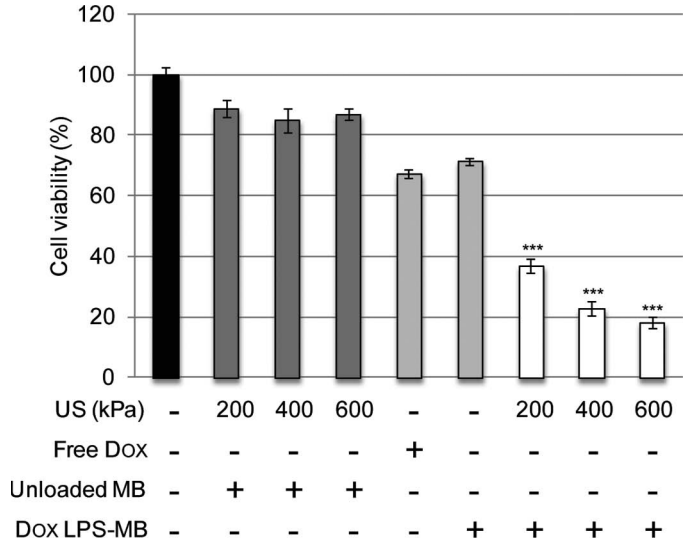

Fig. 6. Enhancement of doxorubicin (DOX)-induced cell death by ultrasound combined with DOX liposome-loaded microbubbles. U-87 MG cells were incubated with 3 μg/mL doxorubicin alone (Free DOX), or with DOX liposome-loaded microbubbles alone (DOX LPS-MB) or combined with ultrasound at 200, 400, and 600 kPa for 30 s. Forty-eight hours after the treatment, cell viability was measured by an MTT assay. Data expressed as mean ± SEM was calculated from five independent experiments. Statistical analysis was performed using the nonparametric Mann–Whitney test. Significance was defined as $p < 0.05$ ($^{*}p < 0.05$, $^{**}p < 0.01$, and $^{***}p < 0.001$).

the DOX was used to directly measure cellular uptake, fluorescence intensity being directly proportional to the internalized amount of DOX. The insonation of U-87 MG glioblastoma cells at 600 kPa (i.e., optimal acoustic pressure for cell viability) with the unloaded microbubbles did not show an increase in the fluorescence intensity (solid line) as shown in Fig. 8. The result is similar to that obtained with untreated cells (data not shown). The treatment of U-87 MG cells with the DOX liposome-loaded microbubbles alone induced a shift of the histogram to the right (dashed line). This result can be explained by the intracellular DOX leakage from DOX-liposomes incorporated by U-87 MG cells. The combination of ultrasound with DOX liposome-loaded microbubbles induced an additional shift of the histogram to the right (short-dashed red histogram). This result suggests that the cellular uptake of DOX by U-87 MG was significantly ($^{*}p < 0.05$) higher in the cells treated with ultrasound and DOX liposome-loaded microbubbles than in the cells treated with DOX liposome-loaded microbubbles alone. These results confirm that the combination of DOX liposome-loaded microbubbles with ultrasound induced an enhancement of free DOX uptake by U-87 MG cells.

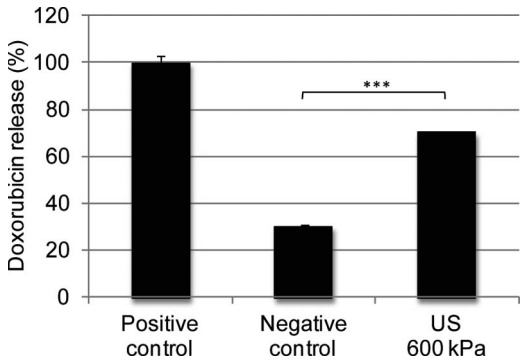

Fig. 7. Enhancement of doxorubicin (DOX) release from DOX liposome-loaded microbubbles after insonation. DOX liposome-loaded microbubbles were incubated with (positive control) or without (negative control) Triton X-100 at 10% v/v in OptiMEM-1% fetal calf serum. In addition, these same microbubbles were insonated at the optimal acoustic pressure of 600 kPa. Data expressed as mean ± standard error of the mean (SEM) was calculated from five independent experiments. Statistical analysis was performed using the nonparametric Mann–Whitney test. Significance was defined as $p < 0.05$ ($^{*}p < 0.05$, $^{**}p < 0.01$, and $^{***}p < 0.001$).

IV. Discussion

The present study examined the imaging and therapeutic properties of DOX liposome-loaded microbubbles for ultrasound-induced delivery of DOX under diagnostic ultrasound guidance. We have shown that when interrogated with low nondestructive MI, these microbubbles scatter sufficient signal for nonlinear ultrasound imaging and can therefore be imaged in real time and tracked *in vivo* (Fig. 4). Loading of the microbubbles with DOX liposomes has no apparent effect on the acoustic properties of the microbubbles other than slightly increasing the destruction threshold (Fig. 5). The therapeutic evaluation of these microbubbles showed that ultrasound insonation of the DOX liposome-loaded microbubbles induced a much higher glioblastoma cell death than treatment with free DOX or DOX liposome-loaded microbubbles alone (Fig. 6). We have demonstrated that the enhanced therapeu-

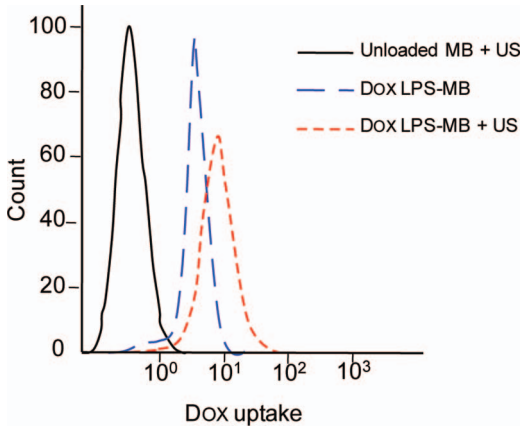

Fig. 8. Enhancement of doxorubicin uptake into U-87 MG cells with doxorubicin (DOX) liposome-loaded microbubbles and ultrasound. U-87 MG cells were incubated with unloaded microbubbles (Unloaded MB + US) or DOX liposome-loaded microbubbles (DOX LPS-MB + US) at the final doxorubicin concentration of 3 μg/mL with ultrasound at 600 kPa. In addition, cells were treated with DOX liposome-loaded microbubbles alone (DOX LPS-MB). Forty-eight hours after the treatment, doxorubicin uptake was measured by flow cytometry. Data expressed as mean ± standard error of the mean (SEM) was calculated from five independent experiments.

tic efficiency is associated with 1) an ultrasound-triggered release of DOX from the DOX liposome-loaded microbubbles (Fig. 8) and 2) an enhanced uptake of free DOX by the cells (Fig. 7). In agreement with our previous data, these results support the hypothesis that sonoporation improves the cellular uptake of free DOX [26], [27], [32]. Indeed, we demonstrated that microbubbles and ultrasound significantly enhanced the cellular uptake of free DOX and the DOX-associated cytotoxicity compared with the treatment with free DOX alone.

Based on the results obtained in the present study, we hypothesized that DOX liposome-loaded microbubbles in combination with ultrasound may significantly improve the *in vivo* effectiveness of targeted DOX delivery under ultrasound imaging guidance. Our data support the idea that the design of a hybrid imaging/therapeutic probe is required to reach this double objective. Following intravenous injection, these smart microbubbles may be tracked *in vivo* using conventional ultrasound contrast imaging modes. Once the tumor microvasculature network is filled with the DOX liposome-loaded microbubbles, a high-intensity therapeutic ultrasound exposure may induce the destruction of microbubbles, promoting 1) the permeation of tumor endothelium, 2) the ultrasound-triggered release, and 3) the extravasation of the free DOX into the endothelial and tumor cells [37]–[39]. The enhanced uptake of DOX in endothelial cells may potentiate the destruction of tumor microvasculature and breakdown the nutrient supply (i.e., oxygen, nutrients, etc.) of the tumor [40]. Because free DOX is more cytotoxic than liposomal DOX [41], the local ultrasound-triggered delivery of free DOX in the tumor may enhance the tumor cell death and tumor eradication. We believe that the use of optimal formulation of DOX liposome-microbubbles (i.e., without free DOX liposomes) might exhibit fewer side effects than free DOX. Thus, in the tissues unexposed to ultrasound, these micro-sized microbubbles would remain intact and there would be no release and extravasation of DOX in these healthy tissues. This assumption remains to be demonstrated in future *in vivo* studies.

In conventional chemotherapy with Doxil, a single therapeutic dose corresponds to 40 mg of DOX for an 80-kg adult patient [41]. The concentration of loaded DOX attached to a single microbubble was estimated to be 5×10^{-9} μg [26]. Based on these figures, a total of 8×10^{12} DOX liposome-loaded microbubbles must be intravenously injected to reach a similar therapeutic dose. However, the recommended diagnostic doses of current contrast agents (e.g., SonoVue and Definity) are, respectively, 10^9 and 10^{10} microbubbles for an 80-kg adult (i.e., about 1000 and 100 times lower than that of DOX liposome-loaded microbubbles required to reach a single therapeutic dose of Doxil). Nevertheless, recent studies have reported a good tolerance with 100- and 1000-fold higher doses of SonoVue and Definity microbubbles in nonhuman primates and patients [42]–[46]. Consequently, the injection of a high dose of DOX liposome-loaded microbubbles could be considered for clinical DOX delivery for therapeutic purposes. However, further preclinical studies might be necessary to identify putative toxicity of high lipid concentrations. In addition, the localized delivery character of this approach would likely require a smaller therapeutic dose than the one used in current chemotherapy protocols. Thus, therapeutic effects can be expected in human at recommended diagnostic microbubble doses.

The enhancement of DOX loading efficiency on the microbubbles and the application of consecutive treatments constitute two other alternative approaches to reach the therapeutic dose of Doxil. The small size of the microbubbles limits the space for DOX loading. Geers *et al.,* reported that the binding of DOX-liposomes on the surface of the microbubbles could increase the amount of loaded doxorubicin [26], although they showed that 600 to 1300 DOX-liposomes nanoparticles are bound per single microbubble; hence, the DOX concentration remains rather limited. Nevertheless, the loading efficiency can be further improved by applying multiple layers of DOX-liposomes around the microbubble shell. Finally, Zhao *et al.*, reported that the repeated treatments of epirubicin and microbubble-assisted ultrasound induced an efficient inhibition of marrow leukemic tumor growth followed by tumor eradication [47]. No side effect associated with this protocol has been reported.

V. Conclusion

Our results demonstrated that DOX liposome-loaded microbubbles have good imaging properties and a high therapeutic potential. Thus, the combination of these smart microbubbles and ultrasound presents a new potential strategy for the ultrasound-triggered DOX delivery under diagnostic ultrasound guidance.

Acknowledgments

The authors thank C. Arnoult (GICC, UMR CNRS 6239, Tours, France), J. Tastet (INSERM UMR-930, Tours, France), and Dr. S. Attucci (INSERM U-1100, Tours, France) for their technical assistance in flow cytometry, spectrophotometry, and spectrofluorimetry, respectively. This project was funded by the EU/FP7 Project Sonodrugs (NMP4-LA-2008-213706).

References

[1] C. Carvalho, R. X. Santos, S. Cardoso, S. Correia, P. J. Oliveira, M. S. Santos, and P. I. Moreira, "Doxorubicin: The good, the bad and the ugly effect," *Curr. Med. Chem.*, vol. 16, no. 25, pp. 3267–3285, 2009.

[2] A. A. Gabizon, "Pegylated liposomal doxorubicin: Metamorphosis of an old drug into a new form of chemotherapy," *Cancer Invest.*, vol. 19, no. 4, pp. 424–436, 2001.

[3] Y. C. Barenholz, "Doxil—The first FDA-approved nano-drug: Lessons learned," *J. Control. Release*, vol. 160, no. 2, pp. 117–134, 2012.

[4] C. L. Bennett and E. A. Calhoun, "Pharmacoeconomics of liposomal anthracycline therapy," *Semin. Oncol.*, vol. 31, no. 6, suppl. 13, pp. 191–195, 2004.

[5] M. E. O'Brien, N. Wigler, M. Inbar, R. Rosso, E. Grischke, A. Santoro, R. Catane, D. G. Kieback, P. Tomczak, S. P. Ackland, F. Oriandi, L. Mellars, L. Alland, C. Tendler; CAELYX Breast Cancer Study Group, "Reduced cardiotoxicity and comparable efficacy in a phase III trial of pegylated liposomal doxorubicin HCl (CAELYX/ Doxil) versus conventional for first-line treatment of metastatic breast cancer," *Ann. Oncol.*, vol. 15, no. 3, pp. 440–449, 2004.

[6] R. R. Patil, S. A. Guhagarkar, and P. V. Devarajan, "Engineered nanocarriers of doxorubicin: A current update," *Crit. Rev. Ther. Drug Carrier Syst.*, vol. 25, no. 1, pp. 1–61, 2008.

[7] R. Deckers and C. T. Moonen, "Ultrasound triggered, image guided, local drug delivery," *J. Control. Release*, vol. 148, no. 1, pp. 25–33, 2010.

[8] A. Fernandez-Fernandez, R. Manchanda, and A. J. McGoron, "Theranostic applications of nanomaterials in cancer: drug delivery, image-guided therapy, and multifunctional platforms," *Appl. Biochem. Biotechnol.*, vol. 165, no. 7–8, pp. 1628–1651, 2011.

[9] A. V. Patil, J. J. Rychak, A. L. Klibanov, and J. A. Hossack, "Real-time technique for improving molecular imaging and guiding drug delivery in large blood vessels: In vitro and ex vivo results," *Mol. Imaging*, vol. 10, no. 4, pp. 238–247, 2011.

[10] V. Frenkel, "Ultrasound mediated delivery of drugs and genes to solid tumors," *Adv. Drug Deliv. Rev.*, vol. 60, no. 10, pp. 1193–1208, 2008.

[11] I. Lentacker, N. Wang, R. E. Vandenbroucke, J. Demeester, S. C. De Smedt, and N. N. Sanders, "Ultrasound exposure of lipoplex loaded microbubbles facilitates direct cytoplasmic entry of the lipoplexes," *Mol. Pharm.*, vol. 6, no. 2, pp. 457–467, 2009.

[12] J.-M. Escoffre, K. Kaddur, M.-P. Rols, and A. Bouakaz, "In vitro gene transfer by electro-sonoporation," *Ultrasound Med. Biol.*, vol. 36, no. 10, pp. 1746–1755, 2010.

[13] K. Iwanaga, K. Tominaga, K. Yamaoto, M. Habu, H. Maeda, S. Akifusa, T. Tsujisawa, T. Okinaga, J. Fukuda, and T. Nishihara, "Local delivery system of cytotoxic agents to tumors by focused sonoporation," *Cancer Gene Ther.*, vol. 14, no. 4, pp. 354–363, 2007.

[14] Y. Ueno, S. Sonoda, R. Suzuki, M. Yokouchi, Y. Kawasoe, K. Tachibana, K. Maruyama, T. Sakamoto, and S. Komiva, "Combination of ultrasound and bubble liposomes enhance the effect of doxorubicin and inhibit murine osteosarcoma growth," *Cancer Biol. Ther.*, vol. 12, no. 4, pp. 270–277, 2011.

[15] J. Wu, "Theoretical study on shear stress generated by microstreaming surrounding contrast agents attached to living cells," *Ultrasound Med. Biol.*, vol. 28, no. 1, pp. 125–129, 2002.

[16] A. A. Doinikov and A. Bouakaz, "Acoustic microstreaming around an encapsulated particule," *J. Acoust. Soc. Am.*, vol. 127, no. 3, pp. 1218–1227, 2010.

[17] C. D. Ohl and B. Wolfrum, "Detachment and sonoporation of adherent HeLa-cells by shock waves-induced cavitation," *Biochim. Biophys. Acta*, vol. 1624, no. 1–3, pp. 131–138, 2003.

[18] C. D. Ohl, M. Arora, R. Ikink, N. de Jong, M. Versluis, M. Delius, and D. Lohse, "Sonoporation from jetting cavitation bubbles," *Biophys. J.*, vol. 91, no. 11, pp. 4285–4295, 2006.

[19] B. D. M. Meijering, L. J. M. Juffermans, A. van Wamel, R. H. Henning, I. S. Zuhorn, M. Emmer, A. M. G. Versteilen, W. J. Paulus, W. H. van Gilst, K. Kooiman, N. de Jong, R. J. P. Musters, L. E. Deelman, and O. Kamp, "Ultrasound and microbubble-targeted delivery of macromolecules is regulated by induction of endocytosis and pore formation," *Circ. Res.*, vol. 104, no. 5, pp. 679–687, 2009.

[20] A. A. Doinikov and A. Bouakaz, "Theoretical investigation of shear stress generated by a contrast microbubble on the cell membrane as a mechanism for sonoporation," *J. Acoust. Soc. Am.*, vol. 128, no. 1, pp. 11–19, 2010.

[21] C. Greis, "Technology overview: SonoVue (Bracco, Milan)," *Eur. Radiol.*, vol. 14, suppl. 8, pp. 11–15, 2004.

[22] T. Yoshida, T. Kondo, R. Ogawa, L. B. Feril Jr., Q. L. Zhao, A. Watanabe, and K. Tsukada, "Combination of doxorubicin and low-intensity ultrasound causes a synergistic enhancement in cell killing and an additive enhancement in apoptosis induction in human lymphoma U937 cells," *Cancer Chemother. Pharmacol.*, vol. 61, no. 4, pp. 559–567, 2008.

[23] V. Frenkel, A. Etherington, M. Greene, J. Quijano, J. Xie, F. Hunter, S. Dromi, and K. C. Li, "Delivery of liposomal doxorubicin (Doxil) in breast cancer tumor model: Investigation of potential enhancement by pulsed-high intensity focused ultrasound exposure," *Acad. Radiol.*, vol. 13, no. 4, pp. 469–479, 2006.

[24] E. Hagtvet, T. J. Evjen, D. R. Olsen, S. L. Fossheim, and E. A. Nilssen, "Ultrasound enhanced antitumor activity of liposomal doxorubicin in mice," *J. Drug Target.*, vol. 19, no. 8, pp. 701–708, 2011.

[25] P. Mohan and N. Rapoport, "Doxorubicin as a molecular nanotheranostic agent: Effect of doxorubicin encapsulation in micelles or nanoemulsions on the ultrasound-mediated intracellular delivery and nuclear trafficking," *Mol. Pharm.*, vol. 7, no. 6, pp. 1959–1973, 2010.

[26] B. Geers, I. Lentacker, N. N. Sanders, J. Demeester, S. Meairs, and S. C. de Smedt, "Self-assembled liposome-loaded microbubbles: The missing link for safe and efficient ultrasound triggered drug-delivery," *J. Control. Release*, vol. 152, no. 2, pp. 249–256, 2011.

[27] J.-M. Escoffre, J. Piron, A. Novell, and A. Bouakaz, "Doxorubicin delivery into tumor cells with ultrasound and microbubbles," *Mol. Pharm.*, vol. 8, no. 3, pp. 799–806, 2011.

[28] C. Y. Lin, J. R. Li, H. C. Tseng, M. F. Wu, and W. L. Lin, "Enhancement of focused ultrasound with microbubbles on the treatments of anticancer nanodrug in mouse tumors," *Nanomedicine*, vol. 8, pp. 900–907, 2012.

[29] M. C. Cochran, J. R. Eisenbrey, M. C. Soulen, S. M. Schultz, R. O. Ouama, S. B. White, E. E. Furth, and M. A. Wheatley, "Disposition of ultrasound sensitive polymeric drug carrier in a rat hepatocellular carcinoma model," *Acad. Radiol.*, vol. 18, no. 11, pp. 1341–1348, 2011.

[30] F. Yan, L. Li, Z. Deng, Q. Jin, and H. Zheng, "Paclitaxel-liposome loaded microbubbles for ultrasound-triggered drug delivery in vitro and in vivo," *J. Acoust. Soc. Am.*, vol. 131, no. 4, p. 3366, 2012.

[31] A. F. Lum, M. A. Borden, P. A. Dayton, D. E. Kruse, S. I. Simon, and K. W. Ferrara, "Ultrasound radiation force enables targeted deposition of model drug carriers loaded on microbubbles," *J. Control. Release*, vol. 111, no. 1–2, pp. 128–134, 2006.

[32] I. Lentacker, B. Geers, J. Demeester, S. C. de Smedt, and N. N. Sanders, "Design and evaluation of doxorubicin-containing microbubbles for ultrasound-triggered doxorubicin delivery: Cytotoxicity and Mechanisms involved," *Mol. Ther.*, vol. 18, no. 1, pp. 101–108, 2010.

[33] M. Lampaskis and M. Averkiou, "Investigation of the relationship of nonlinear backscattered ultrasound intensity with microbubble concentration at low MI," *Ultrasound Med. Biol.*, vol. 36, no. 2, pp. 306–312, 2010.

[34] G. A. Brock-Fischer, M. D. Poland, and P. G. Rafter, "Means for increasing sensitivity in non-linear ultrasound imaging systems." US Patent 5 577 505, Nov. 26, 1996.

[35] M. Averkiou, J. Powers, D. Skyba, M. Bruce, and S. Jensen, "Ultrasound contrast imaging research," *Ultrasound Q.*, vol. 19, no. 1, pp. 27–37, 2003.

[36] M. de Smet, S. Langereis, S. van den Bosch, and H. Grüll, "Temperature-sensitive liposomes for doxorubicin delivery under MRI guidance," *J. Control. Release*, vol. 143, no. 1, pp. 120–127, 2010.

[37] R. Bekeredjian, R. D. Kroll, E. Fein, S. Tinkov, C. Coester, G. Winter, H. A. Katus, and H. Kulaksiz, "Ultrasound targeted microbubble destruction increases capillary permeability in hepatomas," *Ultrasound Med. Biol.*, vol. 33, no. 10, pp. 1592–1598, 2007.

[38] M. R. Böhmer, C. H. T. Chlon, B. I. Raju, C. T. Chin, T. Shevchenko, and A. L. Klibanov, "Focused ultrasound and microbubbles for enhanced extravasation," *J. Control. Release*, vol. 148, no. 1, pp. 18–24, 2010.

[39] S. M. Stieger, C. F. Caskey, R. H. Adamson, S. Qin, F. R. E. Curry, E. R. Wisner, and K. W. Ferrara, "Enhancement of vascular permeability with low-ferquency contrast-enhanced ultrasound in the chorioallantoic membrane model," *Radiology*, vol. 243, no. 1, pp. 112–121, 2007.

[40] M. S. Gordon, D. S. Mendelson, and G. Kato, "Tumor angiogenesis and novel antiangiogenic strategies," *Int. J. Cancer*, vol. 126, no. 8, pp. 1777–1787, 2010.

[41] S. T. Duggan and G. M. Keating, "Pegylated liposomal doxorubicin: A review of its use in metastatic breast cancer, ovarian cancer, multiple myeloma and AIDS-related Kaposi's sarcoma," *Drugs*, vol. 71, no. 18, pp. 2531–2558, 2011.

[42] T. Fritz, M. McKeon, and E. Unger, "Preclinical studies of MRX-115: Safety evaluations of myocardium perfusion agent," *Acad. Radiol.*, vol. 3, suppl. 2, pp. S185–S187, 1996.

[43] S. E. Grauer, G. Sutherland, and T. Fritz, "Safety and echo contrast efficacy of multiple doses of Aerosomes MRX-115 in a phase

I clinical trial," *in AHA, 69th Scientific Sessions*, 1996, Abs. 1857, *Circulation*, vol. 94, pp. I316–I319.
[44] D. Bokor, "Diagnostic efficacy of SonoVue," *Am. J. Cardiol.*, vol. 86, no. 4A, pp. 19G–24G, 2000.
[45] D. Bokor, J. B. Chambers, P. J. Rees, T. G. Mant, F. Luzzani, and A. Spinazzi, "Clinical safety of SonoVue, a new contrast agent for ultrasound imaging, in healthy volunteers and in patients with chronic obstrutive pulmonary disease," *Invest. Radiol.*, vol. 36, no. 2, pp. 104–109, 2001.
[46] E. C. Unger, T. Porter, W. Culp, R. Labell, T. Matsunaga, and R. Zutshi, "Therapeutic applications of lipid-coated microbubbles," *Adv. Drug Deliv. Rev.*, vol. 56, no. 9, pp. 1291–1314, 2004.
[47] Y. Y. Zhao, C. T. Lu, Z. C. Zhou, Z. Jin, L. Zhang, C. Z. Sun, Y. Y. Xu, H. S. Gao, J. L. Tian, F. H. Gao, Q. Q. Tang, W. Li, Q. Xiang, X. Li, and W. F. Li, "Enhancing chemotherapeutic drug inhibition on tumor growth by ultrasound: An in vivo experiment," *J. Drug Target.*, vol. 19, no. 2, pp. 154–160, 2011.

Jean-Michel Escoffre earned his M.Sc. degrees in vectorology, gene therapy, vaccinology, and cell biophysics in 2005 and 2006 from the University Paul Sabatier, Toulouse, France. He obtained his Ph.D. degree in cell biophysics in 2010 from the Institute of Pharmacology and Structural Biology (CNRS, UMR 5089) of the University Paul Sabatier. He is currently pursuing postdoctoral research at the Institute of Imaging and Brain of the French Institute for Health and Medical Science (INSERM, UMR 930) in Tours, France. His main research interests lie in the fields of gene and drug delivery by therapeutic ultrasound.

Christophoros Mannaris graduated from the Bioengineering Department of the University of California, San Diego. In 2008, he earned his M. Sc. degree from the Department of Mechanical and Manufacturing Engineering, University of Cyprus, where he is now pursuing his Ph.D. degree. His main research interests lie in the fields of ultrasound-enhanced drug delivery, microbubble contrast agents, and diagnostic ultrasound.

Bart Geers obtained his M.Sc. degree in pharmaceutical sciences from Ghent University, Belgium, in 2008. In the same year, he started his Ph.D. degree in the laboratory of General Biochemistry and Physical Pharmacy at Ghent University. His doctoral research is focused on the development of drug-loaded microbubbles for ultrasound-assisted drug delivery.

Anthony Novell received his M.Sc. degree in medical imaging technologies in 2007 and his Ph.D. degree in 2011 from the University François Rabelais, Tours, France. He is currently pursuing postdoctoral research at the French Institute for Health and Medical Research (INSERM) in Tours, France. His research focuses on contrast agent imaging, capacitive micromachined ultrasonic transducers (cMUTs), and therapeutic ultrasound.

Ine Lentacker obtained her M.Sc. and Ph.D. degrees in pharmaceutical sciences in 2004 and 2009, respectively, from Ghent University, Belgium. She is currently a postdoctoral fellow at the laboratory of General Biochemistry and Physical Pharmacy at Ghent University. Her postdoctoral research is focused on the development of drug-loaded microbubbles for ultrasound-assisted drug delivery.

Michalakis (Mike) Averkiou (M'98) has been an associate professor in the Department of Mechanical and Manufacturing Engineering of the University of Cyprus since 2005 and was the recipient of the Marie Curie Chair of Excellence of the European Commission (2006–2009). He received B.S., M.S., and Ph.D. degrees in 1987, 1989, and 1994, respectively, all in mechanical engineering with specialization in nonlinear acoustics/biomedical ultrasound, from the University of Texas at Austin. He was a Postdoctoral Fellow at the Applied Physics Laboratory of the University of Washington from 1994 to 1996 and worked on lithotripsy, bubble dynamics, and therapeutic ultrasound. He worked in the Philips Medical Systems R&D department from 1996 to 2005. His current research interests are in the areas of diagnostic ultrasound imaging, microbubble ultrasound contrast agents, quantification of tumor angiogenesis, and ultrasound-induced drug delivery. He has authored or co-authored more than 40 journal articles and conference proceedings, and 4 book chapters. He holds more than 30 U.S. and international patents on diagnostic and therapeutic applications of ultrasound.

Ayache Bouakaz graduated from the Department of Electrical Engineering of the University of Sétif, Algeria. He obtained his Ph.D. degree in 1996 from the Department of Electrical Engineering of the Institut National des Sciences Appliquées de Lyon (INSA Lyon), France. In 1998, he joined the Department of Bioengineering at The Pennsylvania State University in State College, PA, where he worked as a postdoctoral researcher for 1 year. From February 1999 to November 2004, he was employed at the Erasmus University Medical Center, Rotterdam, The Netherlands. His research focused on imaging, ultrasound contrast agents and transducer design. Since January 2005, he has held a permanent position as a director of research at the French Institute for Health and Medical Research, INSERM in Tours, France, where he heads the ultrasound laboratory. His research focuses on imaging and therapeutic applications of ultrasound and microbubbles.